Birkeland Currents and Dark Matter

Donald E. Scott

Dept. of Electrical Engineering (Retired), University of Massachusetts, Amherst, Massachusetts, USA
E-mail: dascott3@cox.net

A straight-forward application of basic electrical definitions and one of Maxwell's divergence equations provide an extension of the Bessel function model of force-free, field-aligned currents (FAC). This extended model offers descriptions of the charge density, electric-field strength, velocity profile, and voltage profile, each as a function of radial value, r, within the cross-section of the FAC structure. The resulting model exhibits an obvious correspondence with the results of the Marklund convection process in plasma filaments. Most importantly, it shows that observed stellar velocity profiles in galaxies are now accurately predicted without invocations of Dark Matter, WIMPs, or MACHOs.

1 Introduction

Kristian Birkeland's hypothesis [1] that Earth's auroras are powered by electric charges flowing from the Sun was shown to be correct in the late 1960's [2]. Since that time there has been a growing interest in the exact structure of those streams. What are the precise shapes and physical properties of these currents that cascade down into Earth's polar regions? NASA calls them "magnetic flux-ropes". A more proper name is Birkeland Currents [3]. The general form of those tube-like flux-ropes is best visualized as being a set of concentric, counter- rotating, cylinders made up of various electric currents and magnetic fields. One mathematical description of these structures is called the "Bessel Function Model". Its derivation was initiated in 1950 by physicist Stig Lundquist [4,5]. This derivation was completed and its physical consequences further defined by Scott in 2015 [6].

2 Force-free plasmas are field-aligned

The mechanism by which each moving charge magnetically affects its neighbors is called the Lorentz magnetic force [7]. If these Lorentz forces can be reduced to zero-value everywhere through out the plasma, then the overall current will proceed placidly with increased structural integrity, and not be diverted from its original direction. If, at every point in the flow, the magnetic-flux, **B**, and the electric-current density, **j**, are aligned in the same direction (thus the adjective "field-aligned"), all disruptive Lorentz forces within the plasma will be eliminated and the system is then termed a "Force-Free, Field-Aligned Current" (FAC).

3 Basic properties of field-aligned currents

The Bessel function model of a FAC explicitly involves only two canonical variables: the magnetic-field, **B**(r), and electric current density **j**(r). The model requires these two vector quantities to be everywhere parallel (non-interacting). Cylindrical coordinates (with fixed unit vectors r, θ, z) are used to describe the resulting shape. Because the flow is assumed to be of unlimited extent in length and have a circular cross-section, the model assumes no variation of either **B** or **j** in the θ, or z directions. The mathematical results of this modeling process are:

$$B_z(r) = B_z(0)\, J_0(\alpha r)\,, \tag{1}$$

$$B_\theta(r) = B_z(0)\, J_1(\alpha r)\,, \tag{2}$$

$$j_z(r) = \frac{\alpha B_z(0)}{\mu}\, J_0(\alpha r)\,, \tag{3}$$

$$j_\theta(r) = \frac{\alpha B_z(0)}{\mu}\, J_1(\alpha r)\,, \tag{4}$$

$$B_r(r) = j_r(r) = 0\,, \tag{5}$$

where J_0 and J_1 are Bessel functions of the first kind and of order zero and one respectively. The physical consequences of these equations are: The magnetic-field, **B**, at any point inside the current stream, has two components, one in the axial, z direction (1), and one in the "wrap-around" or θ direction (2). The vector sum of these two orthogonal components at any point located at a distance r out from the central z-axis is the net resulting magnetic field vector, **B**(r). The same is true about the current density, **j**; it is made up of two orthogonal components (3) and (4) in the same way that **B** is.

Comparing expressions (1) and (3) shows that magnitudes B_z and j_z have the same shape except for a difference in scale (size). The same is true for B_θ and j_θ as seen in expressions (2) and (4). In general, both **B** and **j** take on parallel, concentric spiral shapes.

Expression (5) reveals that neither the magnetic-field nor current density component is radiated (nothing leaves the cylindrical flow in the outward — radial, r — direction). This preserves the structural integrity of the flow over extreme distances, z. A full derivation of these properties and equations (1) through (5) is contained in Scott's 2015 paper [6].

4 Extension of the Bessel function FAC model

The only physical quantities modeled in the original Bessel function FAC analysis are magnetic-field vector, **B**, and electric current density vector, **j**. But,if there are electric currents present, there must also be electric charges present to create those currents. If there are electric charges in a given region, there may also be electric-fields.

By extending the Bessel function FAC model, the goal of this paper is to determine:

- The scalar charge density profile, $\rho(r)$, that exists within the FAC.

- The electric-field vector, $E(r)$, that may result from this $\rho(r)$ in the FAC.

- The scalar voltage profile, $V(r)$, that may exist over any cross-section of the FAC.

- Whether the Bessel function FAC model is consistent with the Marklund Convection mechanism.

- The extent to which observed stellar rotational profiles in galaxies are explicable by physical properties of the FAC without invoking the presence of hypothetical dark matter.

5 Components of an electric current density

At every point within a FAC, a single current density vector, $\mathbf{j}(r)$, is assumed to exist. It is a vector quantity. Both the magnitude and the direction of this vector will vary only as the radial distance, r, of the point changes. There is no variation of current density or magnetic field with either z or θ.

A way to visualize this $\mathbf{j}(r)$ structure is the following: if one looks inward toward the central z-axis of the flow from any point, r,and then backs away, outward, with increasing distance from the axis, the net current density vector, $\mathbf{j}(r)$, will appear to rotate smoothly clockwise, and its magnitude will gradually decrease (as $1/\sqrt{r}$). This fact (the monotonic decrease of total current density with $1/\sqrt{r}$) is of significant importance in what follows. See figure 1.

The SI dimensional units of an electric current density, $\mathbf{j}(r)$, are Amperes per square meter. [i.e., the number of Amperes of current that are passing through a unit area determines the value of the "current density" there.]

1. The charge density, $\rho(r)$, describes how much charge is contained in a unit volume located at point r. Therefore its SI units are Coulombs per cubic meter (C/m³).

2. The velocity, $\mathbf{v}(r)$, of this unit volume is the second factor. A one Ampere current is defined as being one Coulomb moving past an observation point each second. SI units of velocity are m/sec.

Therefore the current density at any point, r, is given by
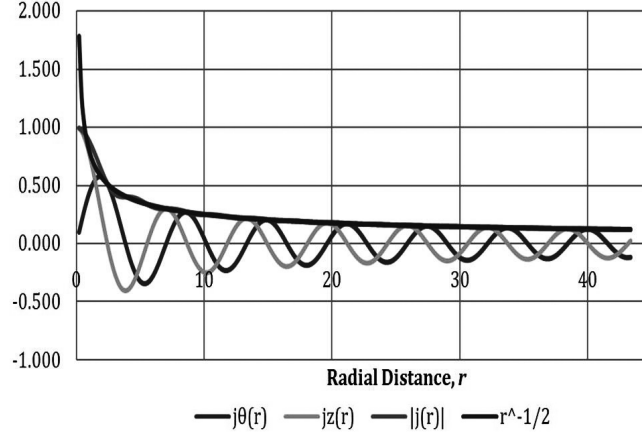
$$\mathbf{j}(r) = \rho(r)\mathbf{v}(r)\,, \tag{6}$$

Fig. 1: Current density and its two components. The magnitude of the total current density varies as $1/\sqrt{r}$.

$$j = \frac{\text{C}}{\text{m}^3}\frac{\text{m}}{\text{s}} = \frac{\text{C/s}}{\text{m}^2} = \frac{\text{A}}{\text{m}^2}\,. \tag{7}$$

In expression 6, $\mathbf{j}(r)$ and $\mathbf{v}(r)$ are both vector quantities and, since $\rho(r)$ is a scalar, it follows that $\mathbf{j}(r)$ and $\mathbf{v}(r)$ are collinear (parallel). Thus the charge density, $\rho(r)$, is defined as being the ratio of the magnitude of the current density vector at point r divided by the magnitude of the velocity vector at that same point. Therefore

$$\rho(r) = \frac{|\mathbf{j}(r)|}{|\mathbf{v}(r)|}\,. \tag{8}$$

Note that in the numerator of (8) it is the *magnitude of the total vector sum* of the current density that is used. The vector components, $j_z(r)$ and $j_\theta(r)$ each vary with r with their oscillating Bessel function shapes, but the magnitude of their vector sum decreases smoothly with increasing radius as $1/\sqrt{r}$ (see figure 1). This value of the magnitude of the total current density, $|\mathbf{j}(r)|$, at every point within the FAC is obtained as the sum of its components, (3) and (4), described above. It is evident from that figure that the magnitude of the current density $|\mathbf{j}(r)|$ varies as $1/\sqrt{r}$.

$$|\mathbf{j}(r)| = \sqrt{j_z^2(r) + j_\theta^2(r)}\,. \tag{9}$$

In order to obtain an evaluation of the charge density, $\rho(r)$, in expression (8), it is necessary to obtain a valid expression for $|\mathbf{v}(r)|$.

6 Estimating the velocity profile of a FAC

It has been suggested [8] that galaxies form on and along cosmic Birkeland currents. Consistent with that hypothesis, we assume that the velocity profiles of stars rotating around a galaxy's center have a conformation similar to the FAC on which that galaxy formed. Galactic velocity profiles have
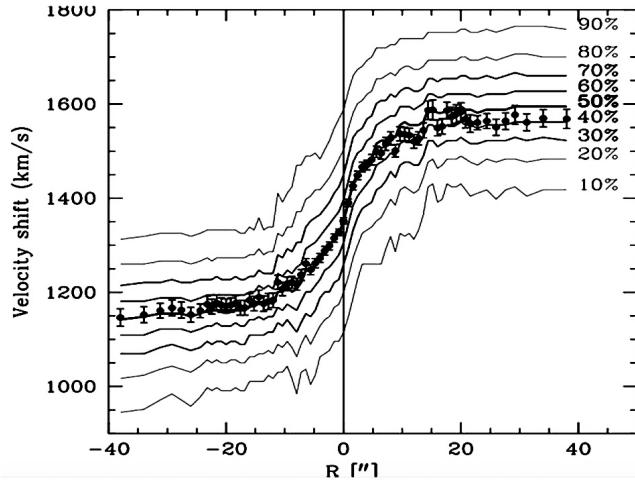
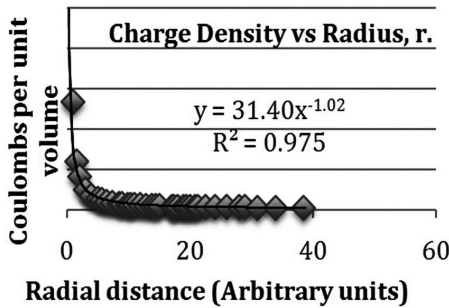Fig. 2: Observed (measured) velocity profile of a typical galaxy. NGC 1620. [9]

Fig. 3: Charge density produced by the known $|\mathbf{j}(r)|$ from the FAC model and the $|\mathbf{v}(r)|$ of the observed galaxy from (8).

been extensively measured both in the past and presently because of their being offered as evidence of the existence of dark-matter, e.g. figure 2.

If using a typical empirically obtained galaxy velocity profile, $|\mathbf{v}(r)|$, in expression (8) results in a realistic charge density, $\rho(r)$, this would constitute supporting evidence for this hypothesis of galaxy formation.

7　A sample stellar velocity profile $|\mathbf{v}(r)|$ for a typical galaxy

The data in figure 2 [9] was sampled (the abscissa and ordinate of each data point was recorded). This empirical data was incorporated into a spreadsheet database. In this way a data series for $|\mathbf{v}(r)|$ was obtained.

Then a numerical data series for $|\mathbf{j}(r)|$ as given by (9) (shown in figure 1) was also entered into the database. Expression (8) was used together with those data sequences for $|\mathbf{j}(r)|$ and $|\mathbf{v}(r)|$ to obtain the charge density, $\rho(r)$. The result is shown in figure 3.

Figure 3 indicates that the observed stellar rotation profile

in this sample galaxy (figure 2) will be correctly produced by the Bessel function model FAC if its internal charge density varies with r as

$$\rho(r) = \frac{k}{r} . \qquad (10)$$

8　Charge density determines the electric-field

One of Maxwell's equations describes the relationship between the electric charge density, $\rho(r)$, at any point, r, and the electric field, $\mathbf{E}(r)$, that diverges outward from any such point.

$$\nabla \cdot \mathbf{E}(r) = \frac{\rho(r)}{\epsilon} . \qquad (11)$$

In this expression, $\rho(r)$ is the electric charge density at the point r and ϵ is the permittivity of the surrounding medium. Therefore the electric-field in a region (such as within this FAC) may be obtained by solving (11) using the $\rho(r)$ arrived at in (10).

The general form of the divergence operator in cylindrical coordinates is

$$Div\,\mathbf{E} = \nabla \cdot \mathbf{E}(r) = \frac{1}{r}\frac{\partial}{\partial r}(rE_r) + \frac{1}{r}\left(\frac{\partial E_\theta}{\partial \theta}\right) + \frac{\partial E_z}{\partial z} . \qquad (12)$$

As before, it was assumed that, in a Birkeland current there is no variation of $\mathbf{E}$ with respect to axial distance z, nor with angular displacement θ, around that axis. There is no preferred location along the unboundedly long z-axis, and there is no angle, θ, around that axis that is preferred over any other. Using these simplifications in (12) and substituting into (11) yields

$$\frac{1}{r}\frac{\partial}{\partial r}(rE_r) = \frac{\rho(r)}{\epsilon} , \qquad (13)$$

$$\frac{\partial}{\partial r}(rE_r) = \frac{r\rho(r)}{\epsilon} , \qquad (14)$$

$$E_r = \frac{1}{\epsilon r}\int_0^r r\,\rho(r)\,dr . \qquad (15)$$

Substituting (10) into (15) and integrating results in

$$E_r(r) = \frac{k}{\epsilon} . \qquad (16)$$

Therefore the electric-field has a constant value across the entire cross-section of the FAC. The force per unit + charge is outward.

9　The voltage profile is determined by the electric-field, $E(r)$

Using the definition of the electric-field,

$$E_r(r) = -\frac{\partial V(r)}{\partial r} , \qquad (17)$$

$$V(r) = -\int_0^r \frac{k}{\epsilon}\,dr = -\frac{kr}{\epsilon} + C. \qquad (18)$$
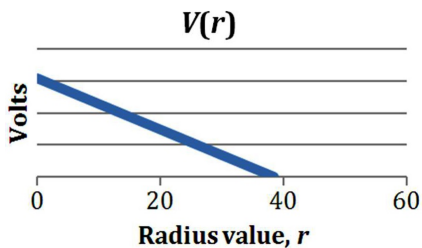
Fig. 4: Voltage profile of cross-section of a FAC.

The constant of integration, C, is chosen such that at the outer boundary of the FAC, $V(R) = 0$. The force per unit charge (16) thus creates a linear, uniformly decreasing voltage profile (18) across the FAC cross-section.

10 Marklund Convection

The voltage profile, $V(r)$, shown in figure 4 is fully consistent with the process known as Marklund Convection [10] wherein elements become sorted radially within a plasma filament according to their ionization potential. Neutral atoms diffuse into the FAC and become ionized due to a temperature gradient which is coolest at the center of the filament and hottest at its outer edge. This temperature gradient is caused by the voltage profile of figure 4 which accelerates ions outward to larger values of r. The turbulence (measured as temperature) of this radial flow at its periphery ionizes high V_i elements more easily than at the lower temperatures found near the center of the filament.

Hannes Alfvén [op. cit.] showed that elements with the lowest ionization potential are brought closest to the axis, and form concentric hollow cylinders whose radii increase with ionization potential. He said, "The drift of ionized matter from the surroundings into the rope means that the rope acts as an ion pump, which evacuates surrounding regions, producing areas of extremely low density."

In 2013 it was reported by Merrifield [11] that the outer rim of a counter-rotating galaxy (NGC 4550) had a collection of hydrogen-rich stars. This prompted him to say these outer stars were younger than the others: "Analysis of the populations of the two separate stellar components shows that the secondary disc has a significantly younger mean age than the primary disc, consistent with later star formation from the associated gaseous material. In addition, the secondary disc is somewhat brighter, also consistent with such additional star formation. However, these measurements cannot be self-consistently modeled by a scenario in which extra stars have been added to initially identical counter-rotating stellar discs, which rules out the Evans and Collett's elegant 'separatrix-crossing' model for the formation of such massive counter-rotating discs from a single galaxy, leaving some form of unusual gas accretion history as the most likely formation mechanism."
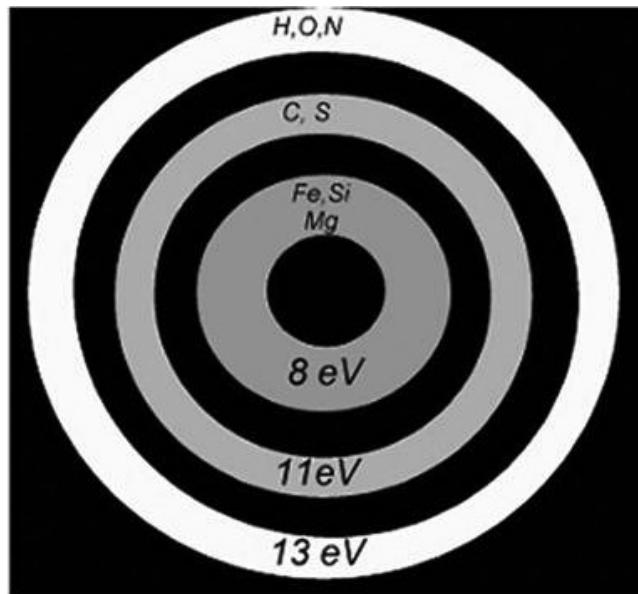

Fig. 5: Elements sorted in a plasma filament in order of their ionization voltage via the Marklund convection process.

Marklund convection stipulates that hydrogen and helium, two elements with the highest ionization voltage, will indeed be found at the outer rim of a plasma filament. The observation of this phenomenon by Merrifield suggests that a Birkeland current is likely to be responsible for the hydrogen-rich band that he discovered.

In 2012 Merrifield [12] had said in his explanation of the presence of these two different counter-rotating populations of stars in NGC 4550 that first, one uni-directional stellar disk formed and then "later on in its life, gas started flowing in, rotating around in the other direction". But, this leaves unanswered the questions of: from where did this new stream of oppositely rotating gas come? And this new gas, being highly collisional, would quickly smash into gas already there and fall into the galactic center. Thus, the question of "from where do the counter rotating stars come" remains unanswered.

In his earlier paper Scott [6] showed that the oscillations in the J_1 Bessel function that controls the spatial behavior of the current density component, j_θ, in a Birkeland Current produces counter-rotating bands in its cross-section (and presumably also in the galaxy it flows into). These bands are analogous to a multi-lane round-about (traffic circle) where adjacent lanes may be going in opposite directions without collisions.

11 Velocity profile predictions of the FAC Bessel model

If it is assumed that the charge density of a typical FAC is similar to the result of expression (10) and figure 3, $\left(\rho(r) \approx \frac{k_1}{r}\right)$, and also that $|\mathbf{j}(r)| = \frac{k_2}{\sqrt{r}}$ as given by the model, then it follows from (8)that the FAC's velocity profile ought to have the

Donald E. Scott. Birkeland Currents and Dark Matter

following functional form:

$$|\mathbf{v}(r)| = \frac{|\mathbf{j}(r)|}{\rho(r)} = \frac{k_2}{k_1} \sqrt{r} \,. \qquad (19)$$

Using the empirical data for our example galaxy (figure 2), we compare this actual observed $|\mathbf{v}(r)|$ data of the example galaxy with our derived velocity profile (19). See figure 6.

12 Results and Comments

One incidental result of this work strongly supports the existence of the voltage profile necessary for Marklund convection to occur in plasma filaments. See sections 9 and 10 above. However, the principal result presented here is the revelation of the actual cause of "anomalous" stellar rotation profiles in galaxies. Since the beginning of space research, most astrophysicists have asserted that electric fields, and currents, are not important in space phenomena [13]. Because of this rejection of electrical science and experimental plasma engineering, all efforts to explain why the outer stars in galaxies revolve around their galactic centers with velocities that, according to Newtonian dynamics, are too high have failed. This fruitless search has lasted for decades [14]. Invisible dark matter (DM) was first proposed by astronomers Jan Oort (1932) and Fritz Zwicky (1933). Subsequently several different types of DM have been hypothesized [15]:

- Cold collisionless dark matter (CCDM) [16];
- Warm dark matter (WDM) [17];
- Strongly self-interacting dark matter (SIDM) [18, 19, 20];
- Repulsive dark matter (RDM) [21];
- Self annihilating dark matter (SADM) [22];
- Fuzzy dark matter (FDM) [23];
- WIMPs Weakly interacting massless particles [24, 25];
- MACHOs Massive (astrophysical) compact halo objects [26, 27];
- Chameleon and Condensed Scalar Fields (not found as of 2015) [28, 29];
- Proposal to modify Newton's Laws [30].

This eighty-five year quest for a dark matter explanation of galactic stellar rotation profiles has produced only null results. Inserting a galaxy's charge density profile into the Birkeland Current Bessel function model [see expression (19)] now provides an elegantly simple answer shown in figure 6. Recently, scientific attention is becoming focused on discoveries of linkages among galaxies previously thought to be isolated from each other. Wide-field telescope observations of the remote universe, have revealed an immense string of galaxies about 300 million light-years long [31]. New research [32, 33, 34] suggests that galaxies are connected to one another with streams of hot thin ionized gas (hydrogen plasma) called the intergalactic medium or IGM.

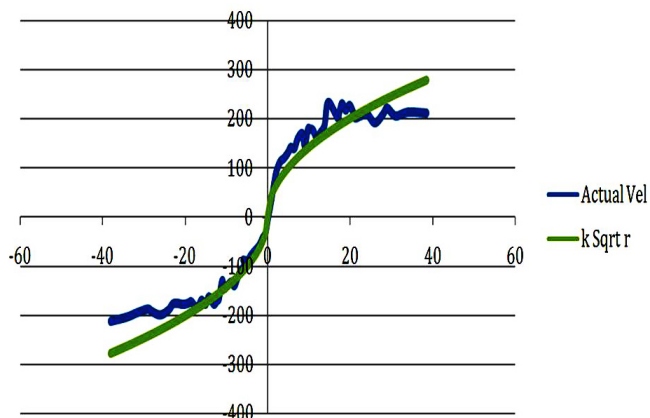### Comparison of Predicted and Actual Stellar Velocity Profiles

Fig. 6: Comparison of the example galaxy's measured velocity profile with the Bessel function model's Sqrt r profile.

Observations show a narrow filament, one million light-years long, flowing into a quasar, perhaps fueling the growth of the galaxy that hosts the quasar. Caltech's new Cosmic Web Imager has already detected one possible spiral-galaxy-in-the-making that is three times the size of our Milky Way [35].

An observation that is "anomalous" is one that is inconsistent with accepted hypotheses. In real science this requires the replacement of the falsified hypothesis, not an eighty-five year hunt for invisible entities that will preserve it. The work being presented here demonstrates that the root cause of the now vast collection of observed "anomalous" galactic stellar rotation profiles is the electrical nature of the Birkeland Currents on which those galaxies have been or are being formed.

Acknowledgment

References

1. Birkeland K. The Norwegian Polaris Expedition 1902-1903. Vol. 1, Sect. 1, Aschehoug, Oslo, 1908.

2. Zmuda A. et. al. Characteristics Of Transverse Magnetic Disturbances Observed At 1100 Kilometers. *Auroral Oval Journal of Geophysical Research*, 1970, v.75, issue 25, 4757.

3. Alfvén H. Cosmic Plasma. Boston, D. Reidel, 1981, pages 16, 15–26, 36.

4. Lundquist S. Magneto-Hydrostatic Fields. *Arch. Fys.*, 1950, v. 2, 361–365.

5. Lundquist S. On the Stability of Magneto-Hydrostatic Fields. *Phys. Rev.*, 1951, v. 83(2), 307–311.

6. Scott D. Consequences Of The Lundquist Model Of A Force-Free Field Aligned Current. *Prog. Phys.*, 2015, v. 10(1), 167–178.

7. Peratt A. Physics Of The Plasma Universe. Springer-Verlag, New York, 1992, pages 43–44, 95, 103, 229. Repprinted in 2015.

8. ICRA, Astronomers find faint strings of galaxies inside empty space. International Center for Radio Astronomy Research, Perth, Western Australia. Published: March 11, 2014. http://www.astronomy.com/news/2014/03/astronomers-find-faint-strings-of-galaxies-inside-empty-space

9. NGC 1620, https://www.aanda.org/articles/aa/full/2004/35/aa0183-04/img97.gif

10. Marklund G. Plasma convection in force-free magnetic fields as a mechanism for chemical separation in cosmical plasma. *Nature*, 1979, v. 277, 370–371.

11. Johnson E., Merrifield M. Disentangling the Stellar Populations in the counter-rotating disc galaxy NGC 4550. *Monthly Notices of the Royal Astronomical Society*, 2013, v. 428(2), 1296–1302; arXiv: 1210.0535 [astro-ph.CO].

12. Merrifield M. Strange Galaxy (NGC 4550). https://www.youtube.com/watch?v=0oie90j989kδt=1sδlist=PLGJ6ezwqAB2a4RP8hWEWAGB9eT2bmaBsyδindex=40 Published 10/2012.

13. Scott D. Real Properties of Electromagnetic Fields and Plasma in the Cosmos. *IEEE Transactions on Plasma Science*, 2007, v. 35(4), 822–827.

14. Scoles S. How Vera Rubin Confirmed Dark Matter. *Astronomy*, October 4, 2016. http://www.astronomy.com/news/2016/10/vera-rubin

15. Ostriker J.P. and Steinhardt P. New Light on Dark Matter. *Science*, 2003, v. 300(5627), 1909–1913.

16. Ma C-P. Are Halos of Collisionless Cold Dark Matter Collisionless? *Phys. Rev. Letters*, 2004, v. 93(2), 021301.

17. Viel M., et al. Constraining warm dark matter candidates including sterile neutrinos and light gravitinos with WMAP and the Lyman-α forest. *Phys. Rev. D*, 2005, v. 71, 063534.

18. Wandelt BD. Self-Interacting Dark Matter, arXiv:astro-ph/0006344.

19. Zavala J. Constraining self-interacting dark matter with the Milky Way's dwarf spheroidals. *Monthly Not. RAS*, 2013, v. 431(1), L20–L24.

20. Hui L., Unitarity bounds and the cuspy halo problem. *Physical Review Letters*, 2001, v. 86, 3467.

21. Fan J. Ultralight Repulsive Dark Matter and BEC. *Physics of the Dark Universe*, 2016, v. 14, 1-126.

22. Natarajan P. Consequences of dark matter self-annihilation for galaxy formation, arXiv:0711.2302 [astro-ph].

23. Is Dark Matter "Fuzzy", Astronomy Now, Chandra X-ray Center press release, 2 May 2017.

24. Kochanek CS., White M. A Quantitative Study of Interacting Dark Matter in Halos. *The Astrophysical Journal*, 2000, v. 543(2).

25. Alcock C. The Dark Halo of the Milky Way. *Science*, 2000, v. 287(5450), 74–79.

26. Alcock C. et al. The MACHO Project: Microlensing Results from 5.7 Years of Large Magellanic Cloud Observations. *The Astrophysical Journal*, 2000, v. 542(1), 281–307.

27. Zeyher A. MACHOs may be out of the running as a dark matter candidate, Astronomy (2016); http://www.astronomy.com/news/2016/08/machos-may-be-out-of-the-running-as-a-dark-matter-candidate

28. Wilkinson R. The search for "dark matter" and "dark energy" just got interesting, Aug. 21, 2015. The Conversation: https://phys.org/news/2015-08-dark-energy.html; also: http://theconversation.com/the-search-for-dark-matter-and-dark-energy-just-got-interesting-46422.

29. Bohua L. Cosmological constraints on Bose-Einstein-condensed scalar field dark matter. *Phys. Rev. D*, 2014, v. 89, 083536.

30. Milgrom M. MOND — A Pedagogical Review. The XXV International School of Theoretical Physics "Particles and Astrophysics — Standard Models and Beyond", Ustron, Poland, September 10-16, 2001. arXiv: astro-ph/0112069

31. Palunas P. Giant Galaxy String Defies Models Of How Universe Evolved, NASA; https://www.nasa.gov/centers/goddard/news/topstory/2004/0107filament.html

32. Fesenmaier K. Astronomers unveil a distant protogalaxy connected to the cosmic web. https://phys.org/news/2015-08-astronomers-unveil-distant-protogalaxy-cosmic.html.

33. Coutinho B. The Network Behind The Cosmic Web. arXiv:1604.03236 [Astro-Ph.Co].

34. Gott J. The Cosmic Web (book). Princeton University Press, forthcoming Jun 2018.

35. Martin D.C. Intergalactic Medium Emission Observations with the Cosmic Web Imager. *Astrophysical Journal* v. 768(2), Art. No. 106. arXiv:1402.4809.